Effect of Geometry and Size of Fiber Reinforced Plastic Deck Profile on Behavior of Bridges

Ali nazemi deylami, [iD] [a,*]

ᵃ Department of Civil Engineering, Takestan Branch, Islamic Azad University, Qazvin, Iran

ABSTRACT

Due to the important role that bridges play in rescue operations after an earthquake, it is necessary that these structures have a higher level of protection against seismic attacks. Earthquake identifies the weak points of the structure and causes the most damage there. Bridges are very vulnerable to these attacks due to their low degree of uncertainty. All bridges built before 1971 were designed with the elastic design method (permissible stress). In this method, the effects of plasticity, section cracking, and plastic deformation are not taken into account. The change of seismic locations based on the principles of elastic design is much less. It is because the structure experiences in a real earthquake, one of the consequences of which is the falling of the decks due to the loss of the support surface. The decision to strengthen the bridge was made when there were many bending and shear cracks on the king beams. The bridge was created. The use of FRP profiles can significantly prevent the damage caused by corrosion and is a good alternative to the traditional methods of strengthening the structure. In this study, a design for the deck of a steel bridge with I beams is presented. The shape of reinforcement using FRP fibers with vinyl ester resins has also been investigated, the effect of the geometry of FRP profiles has been investigated. The presented specifications are optimized to obtain a lasting shape and section, especially for the pultrusion process. FRP materials are light, resistant to corrosion and have high tensile strength. These materials come in different forms and range from multi-layer factory sheets to dry sheets that can be twisted on various structural forms before adding resin, is available. The durability and high tensile strength of FRP materials are among the advantages of these materials. The durability and long-term performance of FRP requires more research, which is ongoing and continues.

1. Introduction

Society has searched continuously for new and better materials for building structures. New materials usually come to the stage due to the necessity to improve structural efficiency and performance. However, new materials in turn provide opportunities to develop new structural forms, and present material scientists and engineers with new challenges. One of the best manifestations of the abovementioned inter-related process is associated with

* Corresponding author. Tel.: +989112435320; e-mail: Nazemideylami@gmail.com.

Fiber Reinforced Polymer (FRP) composite materials in bridge applications to which this research is devoted.

In the past few years, FRP composite bridge deck systems have been experimentally implemented in bridge structures. Worldwide, there are many finished or currently underway FRP deck projects. However, an examination of the published resources shows that proper characterization methods and generally accepted design and analysis procedures of FRP bridge decks have not yet been established. While technical difficulties limit the development of affordable fabrication methods to produce low-cost, large-scale FRP bridge decks, the lack of comprehensive analysis and design codes and guidelines for FRP bridge decks is one of the key reasons that FRP decks have so far been applied only in demonstration projects.

To develop analysis and design guidelines and overcome any potential reluctance to use FRP decks, every potential aspect of deck behavior over its service life should be examined experimentally and analytically. There exist at least two principal characteristics that are of primary importance in FRP bridge deck applications, namely stiffness and strength. The stiffness of an FRP deck is the ability of the deck to resist changes in shape when a load is applied. In FRP deck design, a deflection limit is usually used to consider the deck's stiffness. Deck strength is the deck's ability to resist permanent deflection from applied loads (static, dynamic and environmental loads etc.). The development of analysis and design guidelines is primarily based on the comprehension of the stiffness deflection and strength capacity characteristics of FRP deck systems. Other issues on the use of FRP decks, such as dynamic response, durability, efficiency and structural optimization etc., are also related to the understanding FRP deck stiffness and strength.
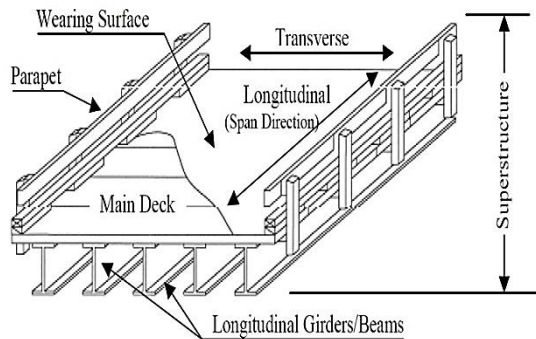

Fig.1 The structure of an engineering bridge [1]

To develop effective FRP deck systems, research pertaining to design and analysis of FRP decks should be fully considered. Analyzing an FRP bridge deck system requires full knowledge of the geometric properties and the material properties. The geometric properties are obtained in the design stage of the deck system. The material and mechanical properties of FRP decks are usually obtained though experimental characterization of the mechanical properties at the coupon, component, and full deck scale levels. In the following section, the development of FRP deck geometric configuration and deck characterization techniques will be reviewed. Also, available analytical models for structural analysis of FRP decks will be presented.

2. Fundamentals of FRP Composite Bridge Decks

A number of terms that are commonly used to describe the upper structure of a bridge are shown in Figure 1. Bridge components more than the bearings are referred to as the superstructure, while the substructure includes all the parts underneath. The main body of the bridge consists of the superstructure, which includes the deck and girders or girders. In this structure, FRP bridge deck is defined as an element made of FRP that transfers shear loads to supports and longitudinal beams.

At present, two major types of FRP deck are currently used in engineering works; Sandwich structure and pultruded structure. Sandwich structures consist of strong, high-stiffness top sheets that can withstand bending loads and have very low density. The core of shear strength is placed between the top sheet and the bottom sheet, which determine the performance of the deck composite. The top sheets are usually made of matte E-glass or a top of polyester or vinyl ester. Core materials include rigid foam or FRP materials in the form of thin-walled cells shown in Figure 2. Cellular materials are the most important materials for structural weight-sensitive applications. Figure 3 shows the sections of the FRP bridge deck.

Pultrusion is an industrial process used to produce continuous parts with a constant cross-section. This process is low cost and with high production volume. This process is similar to the process of metal extrusion, with the difference that instead of pushing the material in the mold, which happens in extrusion, the material is pulled out of the mold, so that the name of this process in English, pultrusion, is also a combination of two words pull (to means pulling) and extrusion. Pultrusion is one of the methods designed to make composites with high mechanical properties that are competitive with traditional and engineering materials. The parts produced by this method have a high volume fraction of fibers; These fibers are mostly placed in the longitudinal direction of the piece. Although with the right weave of fibers, it is possible to have fibers in the transverse direction, but mainly the main properties are in the longitudinal direction. The products obtained from this process have high strength, low weight

and long life, especially in acidic environments. Paltrogen can be used to make any continuous part, provided that it has a constant cross-section and does not have grooves or holes in the direction perpendicular to the tension, such as cans, corners, pipes, rods and similar shapes. The pultrusion process is shown in Figure 4.
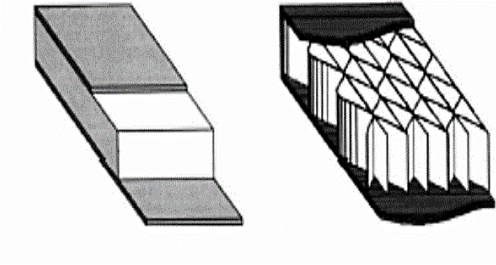

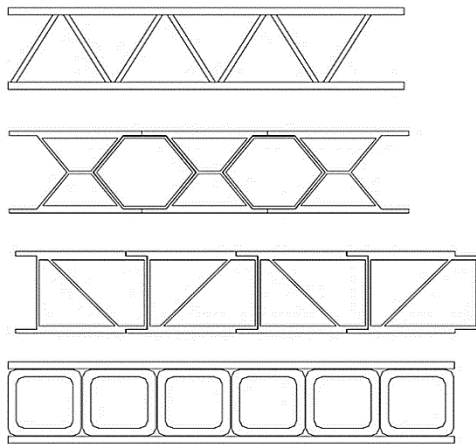Fig. 2. Examples of types of bridge structures with FRP decks [2].
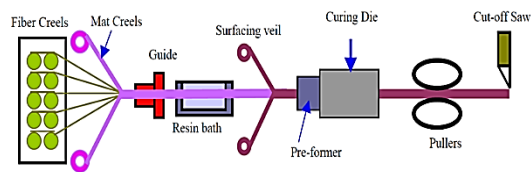

Fig. 3. Types of FRP bridge deck sections [2].

Fig.4. pultrusion process [1]

Table 1 shows the technical comparison between pultruded FRP decks and sandwich sections. As you can see, the sections prepared by the sandwich method are more flexible than the pultruded sections and can create different structures of depth and hardness in the deck. The weight per unit area is usually close to 98 kg/m2, with the exception of the shutter system (Hand/automated lay-up in Table 1), which reduced weight seems to have a higher efficiency in the use of materials. As indicated by the

normalized twist, there is currently no consensus on the amount of deck twist and deflection by manufacturers. Due to the technical difficulties of producing larger parts, some pultruded companies have designed designs that use smaller parts of pultruded modules, such as prismatic or box beams and rectangular plates that are connected to form a large deck.

Table. 1. Available features of FRP decking [1]

Deck systems (Available in the U.S.)	Depth (mm)	[1]Weight (kg/m²)	Cost ($/m²)	[2]Deflection Reported	[3]Deflection Normalized
Sandwich Construction					
Hardcore Composites (VARTM)	152-710	98-112	570-1184	L/785	L/1120
KSCI (Hand/automated lay-up)	127-610	76	700	L/1300	L/1300
Adhesively Bonded Pultrusions					
DuraSpan	194	90	700-807	L/450	L/340
Superdeck	203	107	807	L/530	L/530
EZSpan	229	98	861-1076	L/950	L/950
Strongwell	120-203	112	700	L/605	L/325

[1] Without wearing surface. [2] Assumes plate action. [3] Normalized to HS20+IM for 2.4 m center-to-center span.

Fig. 5. Lab testing configuration [1]

3. Experiment-Based Modeling

Zhou's laboratory model (2002) [1] has been used in the verification for modeling in Abaqus software. In this research, the stiffness and strength of bridge decks built with FRP sections have been investigated. The considered sections are multi-cell sections of FRP bridge decks, which include FRP pultruded sections. In this research, two types of loading have been used to analyze FRP sections. A loading according to the ASSHTO bridge code, which is placed on the bridge as a metal piece, and a loading in the form of truck tires, which applies the actual truck load on the bridge. For validation, loading is considered as a truck load (Figure 5).

The model used in this research is used as the primary model and the basis of modeling in the continuation of the current research work. The section of the FRP profile used

is box section. The cross-section of the laboratory is shown in (figure 6).

The test load was applied to each block by means of a hydraulic cylinder mounted on a load frame, by means of designed loaded pieces. To investigate the local failure of the deck under real truck tire loading, real truck contact patches made of silicone rubber were used. First, a real 22.86 cm (9 inch) truck tire was cut into four pieces. Then the two pieces are filled with silicone rubber gel. After about 24 hours of cooling at room temperature, the rubber pieces filled with tires were ready for testing.

The normal stress distribution of a truck tire and the normal stress distribution of a steel patch are shown in (Figure 7).

However, the normal stress distribution obtained from pressure sensor films indicate that failure tests using steel loading patches are not reliable, since there is no contact at all on most of the deck surface and dominated by contact at the edges. The normal stress distribution of the real truck tire is non-uniform as shown in (Figure 8).

Fig. 6. Box cross section profile [1]
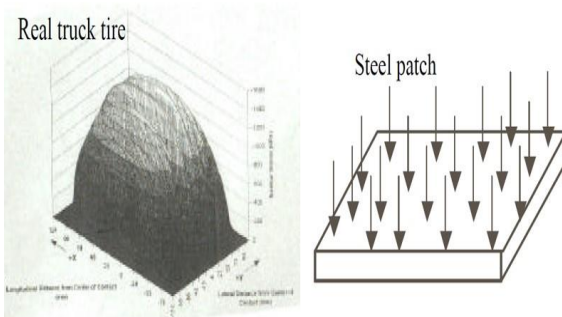
Fig. 7. Normal Stress of a real truck tire and steel Patch [1]

Fig. 8. Normal Stress Distributions of a truck tire and a steel plate using pressure film sensor [1]
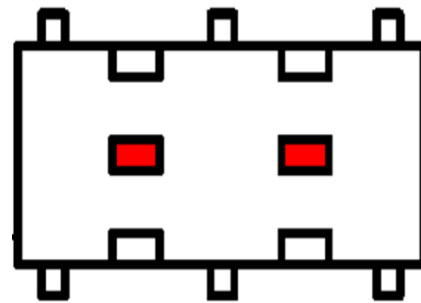

Fig. 9. Normal Stress Distributions of a truck tire [1]

To validate the numerical and laboratory model, loading is used as follows. In this loading, truck tires are loaded in the west and east center of the deck (Figure 9).

The load-displacement diagram is drawn at the points under the load and compared with the laboratory results. (Figure 10).

4. Research method and modeling process in software

The designed cross-section is shown in (Figure 11) [1]. This deck has a length of 4.65 meters and a width of 1.52 meters, which consists of ten box beams (or rectangular tubes) of orthotropic paltrode with dimensions of 15.24 x 15.24 x 0.95 meters. A sheet with a thickness of 0.635 meters at the bottom and a sheet with a thickness of 1.27 meters at the top and 9 steel bolts are placed transversely in the deck. The weight of the deck is about 726 kg with a density of 910.3 kg/m3. To date, no approved specifications and regulations have been proposed for bridges with FRP decks. However, the design and loading ranges in the AASHTO Standard Specification for Highways [AASHTO, 1996] and the AASHTO LRFD Specification, [AASHTO, 1998] for laboratory test models have been used by many FRP deck researchers [1].
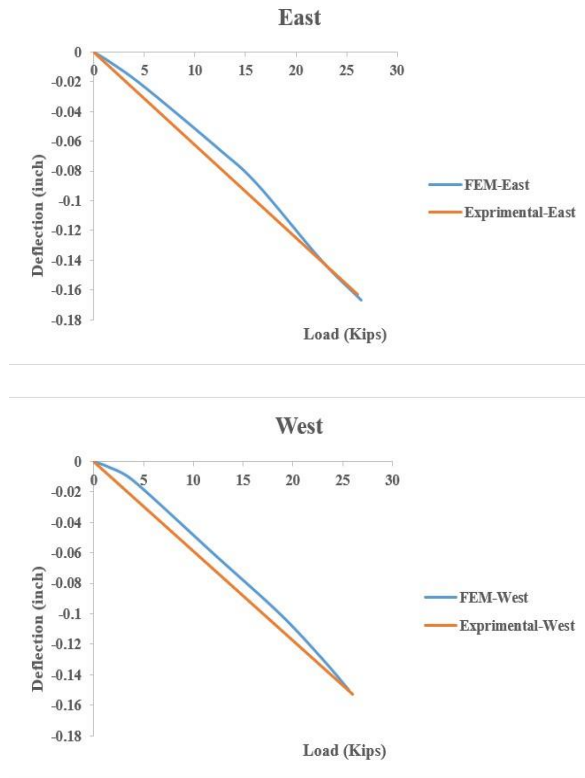
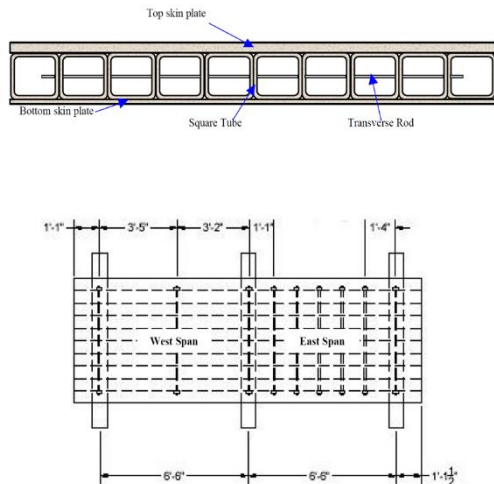Fig.10. Displacement-load curve as central east and west

Fig. 11. Cross section of the deck and transverse bars [1]

According to AASHTO [5] Highway Code, when designing the upper members of a bridge, specified loads are used at critical locations to produce the maximum load effect. The load that produces the greatest stress is known as the design load. Bridge designers can extend the design wheel load over a limited level of the deck by calculating the load effects in a reinforced concrete block. This area is defined as the "tire contact area" and the equation used to calculate it is given in the specification.

The parameters investigated in this research include the change of span length and the change of FRP cross-section and the type of loading (traffic and earthquake). The basic model is the study model of Zhou (2002) [1], which has a box section. It is (Figure 12). The second profile examined in this research, the trapezoidal profile was chosen as the second section for examination (Figure 13).

To check and consider the span length of the bridge deck, once the length of the deck has been checked with three I-shaped supports and another time with four I-shaped supports (Figure 14).

To investigate the performance of FRP deck under different loadings, two types of loading have been considered. Traffic loading according to the AASHTO regulations for trucks and the vertical loading component of the Naghan earthquake, which has been applied to the foundations of the bridge.

Abaqus software provides the possibility of separately modeling the components of a model and then assembling and assembling the components to form the model.
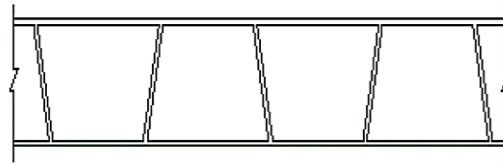

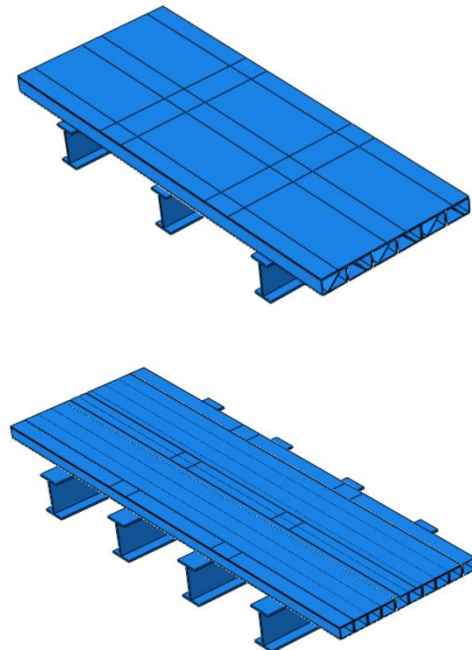Fig. 13.Trapezoidal cross section [3]

Fig. 14. Deck openings used in research

Behavioral characteristics and materials used in FRP deck modeling are according to the table below. Box and trapezoid sections are considered as below (Table 2).

5. Analysis method and loading steps

To perform the analysis, one of three static methods, explicit dynamic and indirect dynamic methods can be used. In dynamic methods in solving the equations, the effect of inertia is also considered and it may spread to immortal waves in the system, for this reason, if these analytical methods are used, it must be ensured that the loading time is considered long enough that the effects dynamic in the system is negligible. Absorbing boundary conditions can also be used to dampen the waves propagated in the system under dynamic movements. On the other hand, because these methods solve dynamic equations in the system, generally the program execution time to reach the results is much longer than static methods.

Table. 2. Material specification in FRP deck modeling

Property	Value
E_{xx} (*psi*)	2.5×10^6
E_{yy} (*psi*)	0.8×10^6
E_{zz} (*psi*)	0.8×10^6
G_{xy} (*psi*)	0.425×10^6
G_{xz} (*psi*)	0.425×10^6
G_{yz} (*psi*)	0.364×10^6
v_{xy}	0.33
v_{xz}	0.33
v_{yz}	0.10

In the places where two separate elements collide during the nonlinear analysis, the characteristics related to the collision should be defined on two surfaces. Otherwise, the collision is not considered in the solution and in the term two elements collide. To define the feature related to the collision, the collision feature must be defined in the software according to the nature of the collision of the elements. In normal collisions, the collision surface has a tangential and frictional behavior. The use of contact behavior in modeling gives the ability to simulate collision and separation of two surfaces in tension.

The loaded areas of the deck are shown in (Figure 15). Loading mode 2-5 is used to simulate truck axle load. Loading modes 1-4 and 3-6 are used to simulate load axis with the expectation of generating more stresses in the northwest and northeast and southwest and southeast

regions for modes 1-4 and 3-6. Mode 2 and Mode 5 will be the loading locations for the failure tests.

The principles of live load loading have been carried out according to the regulations of AAshto [5]. In this research, a 90-ton truck load has been loaded on the bridge. The considered loading mode is the most critical loading mode on the bridge according to the study. According to the width of 10 meters of the crossing and compliance with the distances mentioned in the regulations, the number of crossing lanes for this truck is considered to be 3.

Another mode of loading considered for the current research is earthquake loading, which is chosen as cyclic loading for the current research. Earthquake in the form of acceleration-time entered vertically at the bridge supports. Also, the supports at the place of connection to the bases are considered as holders.
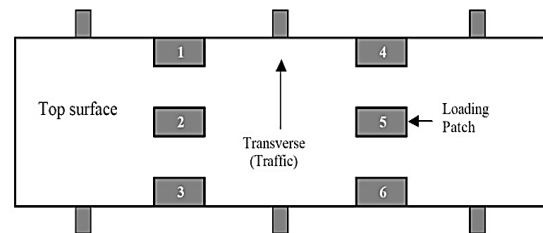

Fig. 15. Deck loaded areas [1]

6. Modeling with Abaqus finite element software

The current research has been carried out with the aim of investigating bridges with FRP decks. The investigated parameters include the type of FRP section, the length of the bridge spans, the type of loading (traffic and earthquake). In Table 3, the investigated models are named.

As can be seen in the table above, the number of models under review is 8 models. To check the performance of the FRP bridge deck under the conditions investigated in this research, the maximum vertical load and displacement diagrams of the deck and the von Mises stress contours of the models have been examined and the results of the models have been compared with each other to obtain the appropriate cross-section and span.

Figure 16 shows the stress versus time diagram for model A-1. This diagram is drawn for the maximum stress developed in FRP sections during loading time. As can be seen in the diagram, the maximum compressive stress is 130 and the tensile stress is 600 MPa.
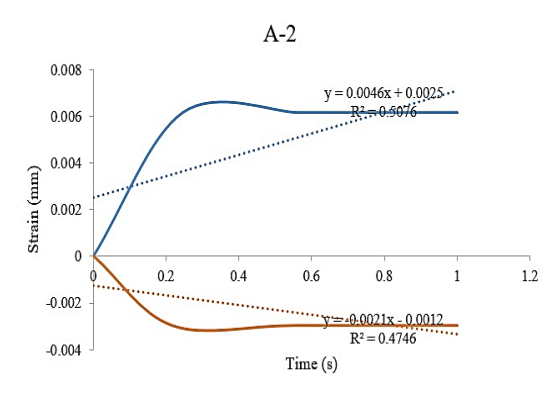
Figure 17 shows the strain versus time diagram for model A-1. This graph is plotted for the maximum strain developed in FRP sections during loading time. As can be

seen in the diagram, the maximum compressive strain is 5.37 and the tensile strain is 0.58 mm.

In figure 18, the contour of von Mises stress created in the I-shaped supports of model A-1 is drawn. As can be seen in the figure, the highest von Mises stress created is equal to 231 MPa and the lowest von Mises stress is equal to 0.66 MPa.

Table. 3. Introducing the investigated model

Load type	The number of openings	FRP section	MODEL
Traffic	3	BOX	A-1
Traffic	4	BOX	A-2
Earthquake	3	BOX	A-3
Earthquake	4	BOX	A-4
Traffic	3	Trapezius	B-1
Traffic	4	Trapezius	B-2
Earthquake	3	Trapezius	B-3
Earthquake	4	Trapezius	B-4
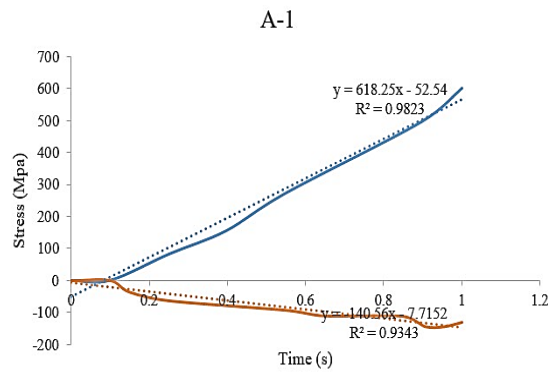
Fig. 16.Stress diagram of model A-1
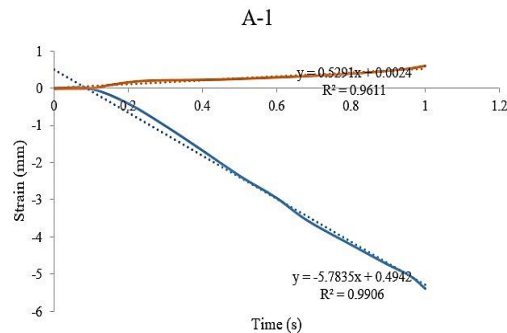
Fig. 17.Strain diagram of model A-1
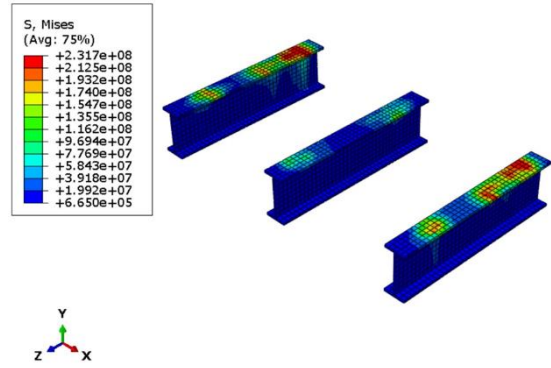
Fig. 18. Von Mises stress contour of model A-1 supports
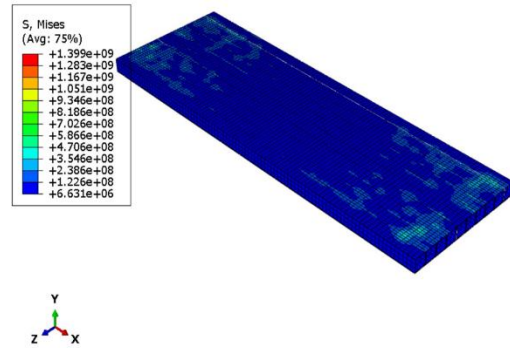
Fig. 19. Von Mises stress contour of FRP sections model A-1
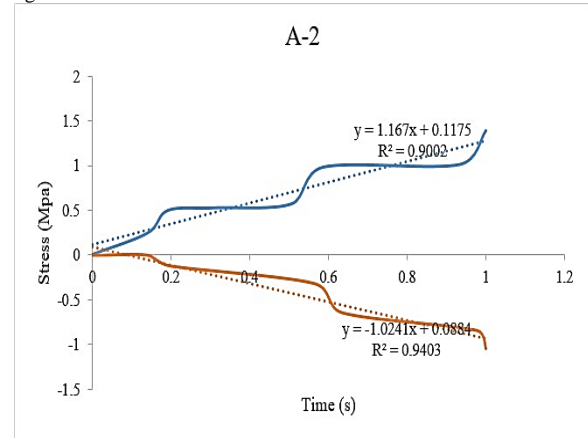
Fig. 20.Stress diagram of model A-2

Figure 19 shows the von Mises stress contour created in the FRP sections of the A-1 deck. As seen in the figure, the highest von Mises stress created in FRP sections is equal to 1399 MPa and the lowest von Mises stress is equal to 6.63 MPa.

Figure 20 shows the stress versus time diagram for model A-2. This diagram is drawn for the maximum stress developed in FRP sections during loading time. As can be seen in the diagram, the maximum compressive stress is 1.05 and the tensile stress is 1.4 MPa.
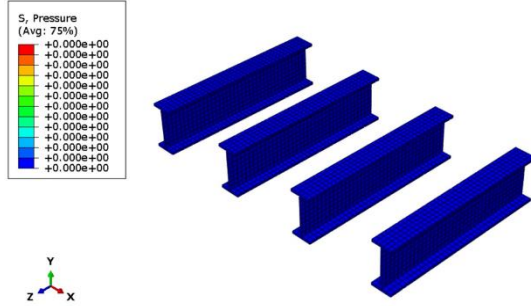
Fig. 21.Strain diagram of model A-2
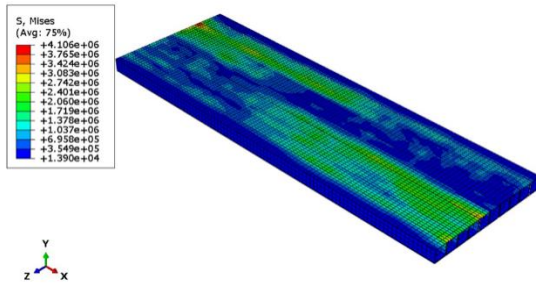

Fig. 22. Von Mises stress contour of model A-2 supports

Fig. 23. Von Mises stress contour of FRP sections model A-2

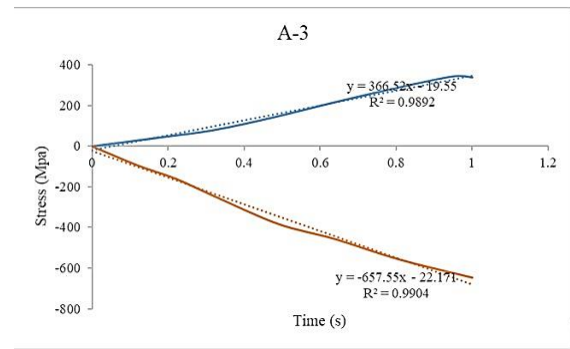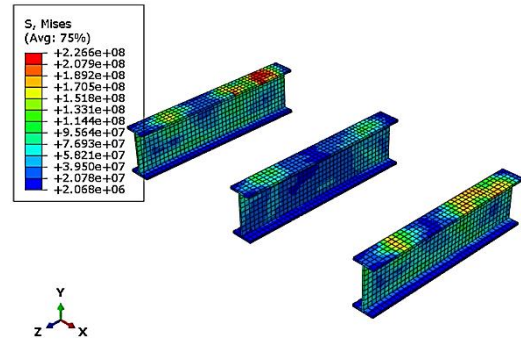Fig. 24.Stress diagram of model A-3

Fig. 25.Strain diagram of model A-3

Fig. 26. Von Mises stress contour of model A-3 supports

Figure 21 shows the strain versus time diagram for model A-2. This diagram is drawn for the maximum strain developed in FRP sections during loading time. As can be seen in the diagram, the maximum compressive strain is 0.003 and the tensile strain is 0.006 mm.

In figure 22, the contour of von Mises stress created in the I-shaped supports of model A-2 is drawn. As can be seen in the figure, by reducing the length of the opening and increasing the supports, there is no significant stress due to the traffic load in the supports.

Figure 23 shows the von Mises stress contour created in the FRP sections of the A-2 deck. As seen in the figure, the highest von Mises stress created in FRP sections is equal to 4.1 MPa and the lowest von Mises stress is equal to 0.013 MPa.

Figure 24 shows the stress versus time diagram for model A-3. This diagram is drawn for the maximum stress developed in FRP sections during loading time. As can be seen in the diagram, the maximum compressive stress is equal to 646 and the tensile stress is equal to 343 MPa.
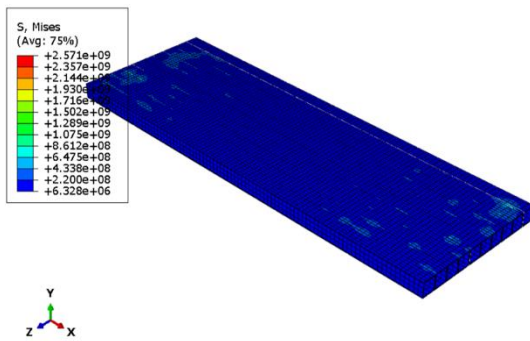
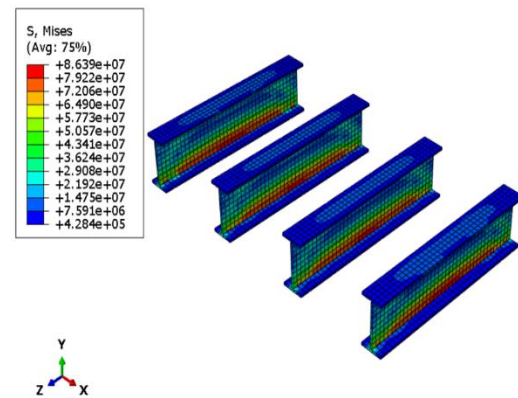Fig. 27. Von Mises stress contour of FRP sections model A-3

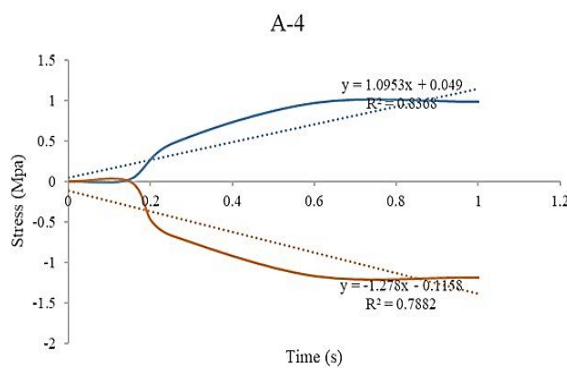Fig. 30. Von Mises stress contour of model A-4 supports
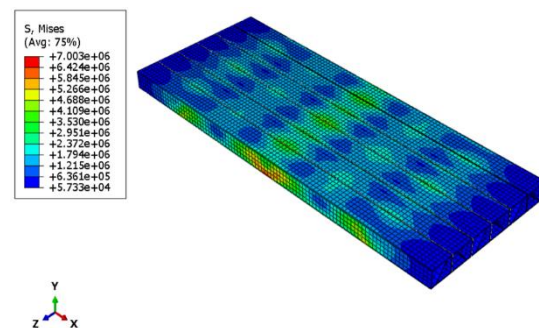

Fig.28.Stress diagram of model A-4

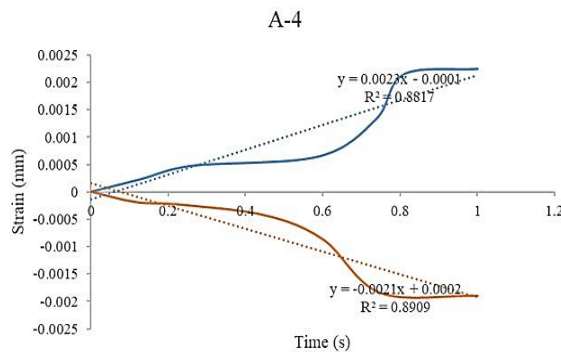Fig. 31. Von Mises stress contour of FRP sections model A-4
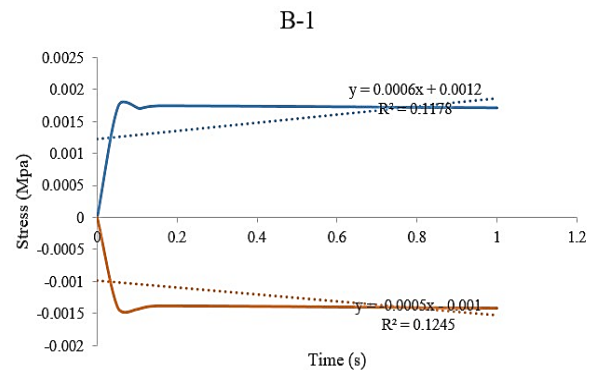

Fig. 29.Strain diagram of model A-4

Fig. 32.Stress diagram of model B-1

Figure 25shows the strain versus time diagram for model A-3. This diagram is drawn for the maximum strain developed in FRP sections during loading time. As can be seen in the diagram, the maximum compressive strain is 0.21 and the tensile strain is 4.09 mm.

In Figure 26, the contour of the von Mises stress created in the I supports of the A-3 model is drawn. As can be seen in the figure, the highest von Mises stress created is equal to 226 MPa and the lowest von Mises stress is equal to 2.06 MPa.

Figure 27 shows the von Mises stress contour created in the FRP sections of the A-3 deck. As seen in the figure, the highest von Mises stress created in FRP sections is equal to 2571 MPa and the lowest von Mises stress is equal to 6.32 MPa.

Figure 28 shows the graph of stress versus time for model A-4. This diagram is drawn for the maximum stress developed in FRP sections during loading time. As can be seen in the diagram, the maximum compressive stress is 1.18 and the tensile stress is 0.98 MPa.
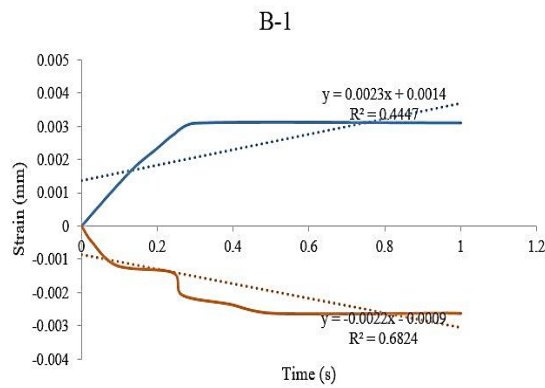
B-1
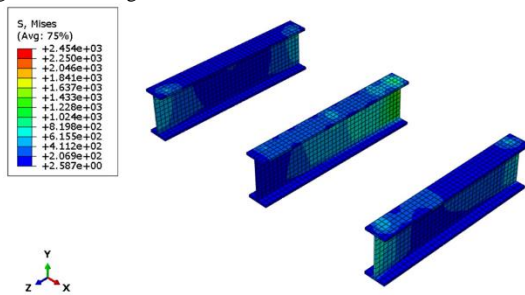

Fig. 33.Strain diagram of model B-1

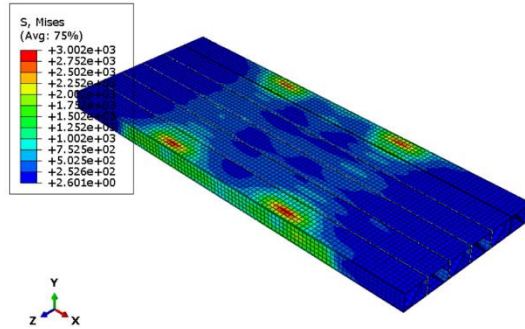Fig. 34. Von Mises stress contour of model B-1 supports

Fig. 35. Von Mises stress contour of FRP sections model B-1

B-2

Fig. 36.Stress diagram of model B-2

B-2

Fig. 37.Strain diagram of model B-2
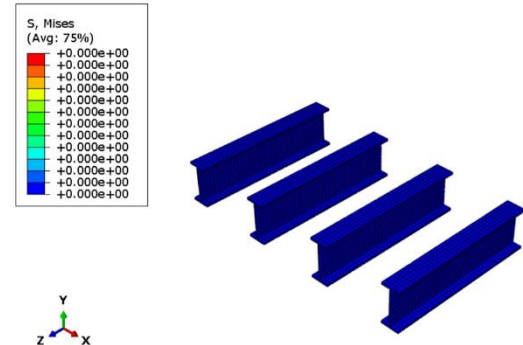
Fig.38. Von Mises stress contour of model B-2 supports

Figure 29 shows the strain versus time diagram for model A-4. This diagram is drawn for the maximum strain developed in FRP sections during loading time. As can be seen in the diagram, the maximum compressive strain is 0.0018 and the tensile strain is 0.0022 mm.

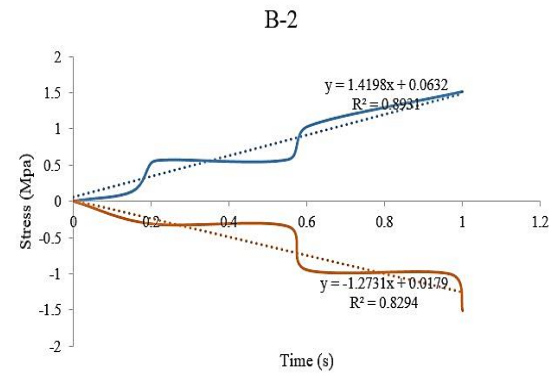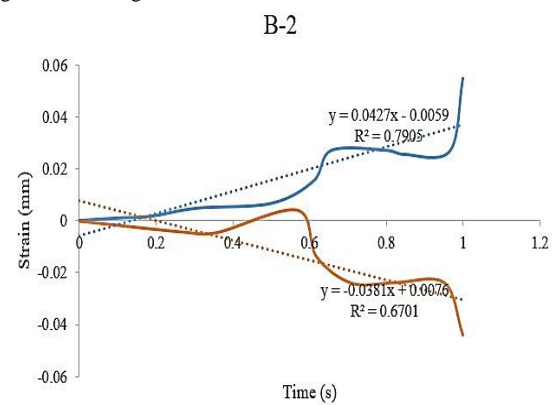In Figure 30, the contour of the von Mises stress created in the I supports of the A-4 model is drawn. As seen in the figure, the highest von Mises stress created is equal to 86 MPa and the lowest von Mises stress is equal to 1.48 MPa.

Figure 31 shows the von Mises stress contour created in the FRP sections of the A-4 deck. As seen in the figure, the highest von Mises stress created in FRP sections is equal to 7 MPa and the lowest von Mises stress is equal to 0.05 MPa.
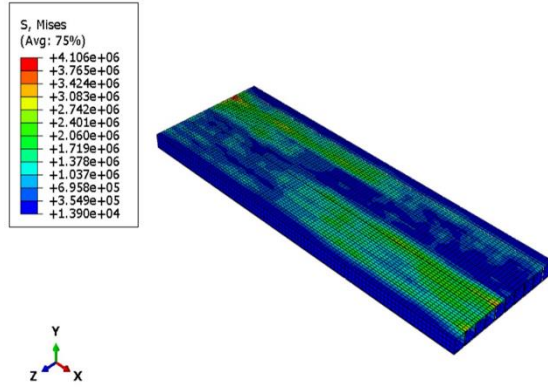
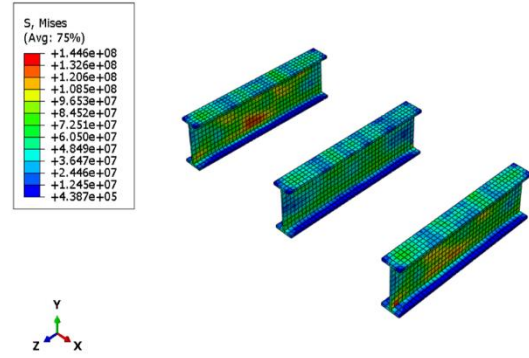Fig.39. Von Mises stress contour of FRP sections model B-2

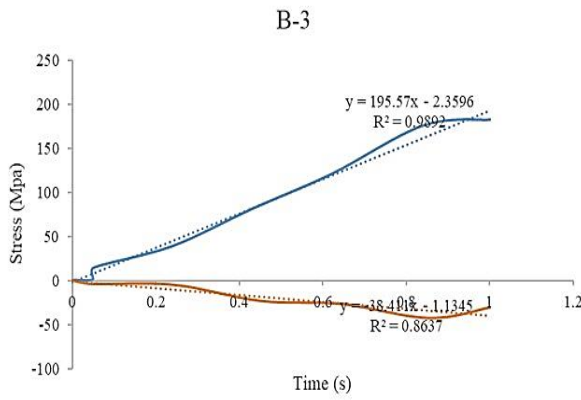Fig.42. Von Mises stress contour of model B-3 supports
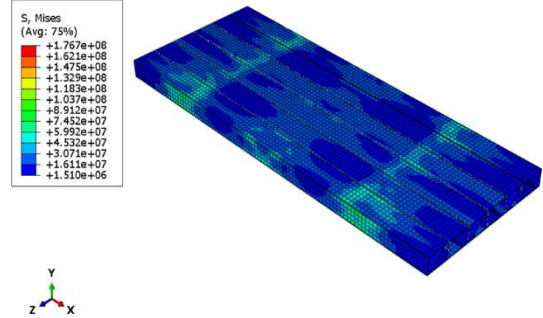

Fig. 40.Stress diagram of model B-3

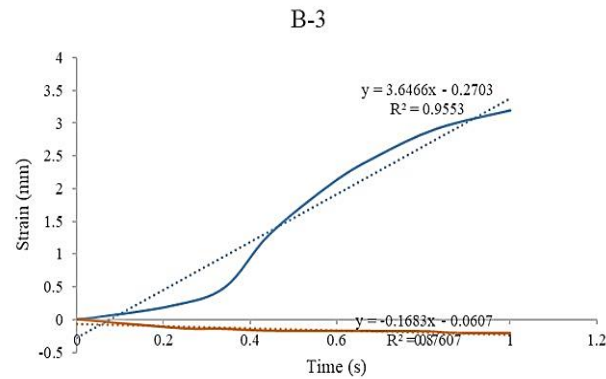
Fig.43. Von Mises stress contour of FRP sections model B-3
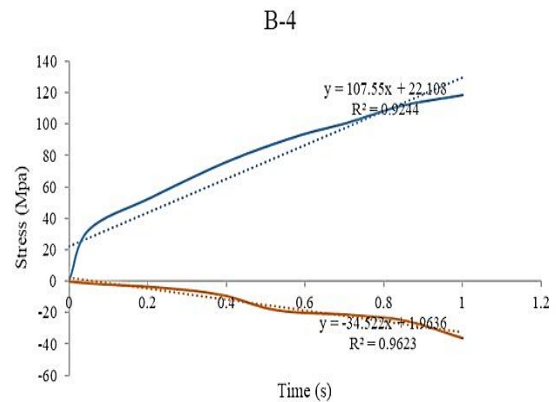

Fig. 41.Strain diagram of model B-3

Fig. 44.Stress diagram of model B-4

Figure 32 shows the stress versus time diagram for model B-1. This diagram is drawn for the maximum stress developed in FRP sections during loading time. As can be seen in the diagram, the maximum compressive stress is equal to 0.0014 and the tensile stress is equal to 0.0017 MPa.

Figure 33 shows the strain versus time diagram for model B-1. This diagram is drawn for the maximum strain

developed in FRP sections during loading time. As can be seen in the diagram, the maximum compressive strain is equal to 0.0026 and the tensile strain is equal to 0.003 mm.

Figure 34 shows the contour of the von Mises stress created in the I-shaped supports of model B-1. As seen in the figure, the highest von Mises stress created is equal to 2.45 k Pa and the lowest von Mises stress is equal to 0.66 Pascal.

Figure 35 shows the contour of the von Mises stress created in the FRP sections of the model B-1 deck. As can be seen in the figure, the highest von Mises stress created in FRP sections is equal to 3 kilopascals and the lowest von Mises stress is equal to 2.6 Pa.

Figure 36 shows the stress versus time diagram for model B-2. This diagram is drawn for the maximum stress developed in FRP sections during loading time. As can be seen in the diagram, the maximum compressive stress is equal to 1.5 and the tensile stress is equal to 1.51 MPa.

Figure 37 shows the strain versus time diagram for model B-2. This diagram is drawn for the maximum strain developed in FRP sections during loading time. As can be seen in the diagram, the maximum compressive strain is 0.043 and the tensile strain is 0.054 mm.

In Figure 38, the contour of the von Mises stress created in the I-shaped supports of the B-2 model is drawn. As it can be seen in the figure, by reducing the length of the opening and increasing the supports, there is no significant stress due to the traffic load in the supports.
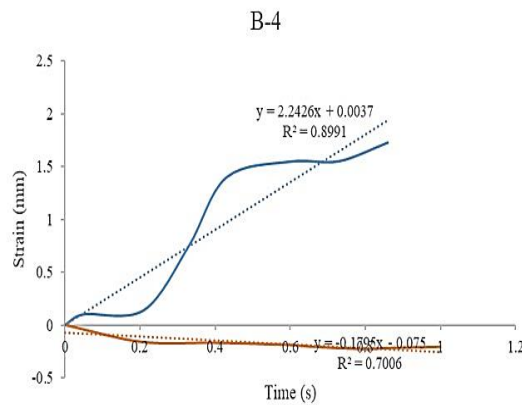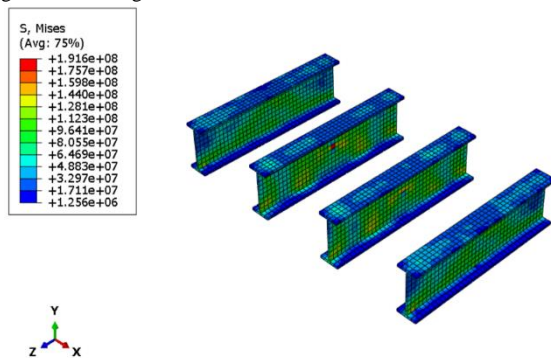

Fig. 45.Strain diagram of model B-4

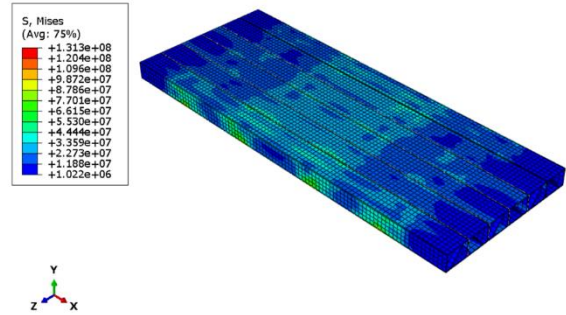

Fig.46. Von Mises stress contour of model B-4 supports

Fig.47. Von Mises stress contour of FRP sections model B-4

Figure 39 shows the von Mises stress contour created in the FRP sections of the model B-2 deck. As can be seen in the figure, the highest von Mises stress created in FRP sections is equal to 4.2 MPa and the lowest von Mises stress is equal to 0.014 MPa.

Figure 40 shows the graph of stress versus time for model B-3. This diagram is drawn for the maximum stress developed in FRP sections during loading time. As can be seen in the diagram, the maximum compressive stress is 42 MPa and the tensile stress is 182 MPa.

Figure 41 shows the strain versus time diagram for model B-3. This diagram is drawn for the maximum strain developed in FRP sections during loading time. As can be seen in the diagram, the maximum compressive strain is 0.207 and the tensile strain is 3.2 mm.

In Figure 42, the contour of the von Mises stress created in the I-shaped supports of the B-3 model is drawn. As seen in the figure, the highest von Mises stress created is equal to 144 MPa and the lowest von Mises stress is equal to 0.43 MPa.

Figure 43 shows the von Mises stress contour created in the FRP sections of the B-3 deck. As seen in the figure, the highest von Mises stress created in FRP sections is equal to 176 MPa and the lowest von Mises stress is equal to 1.51 MPa.

Figure 44 shows the stress versus time diagram for model B-4. This diagram is drawn for the maximum stress developed in FRP sections during loading time. As can be seen in the diagram, the maximum compressive stress is equal to 36 and the tensile stress is equal to 118.25 MPa.

Figure 45 shows the strain versus time diagram for model B-4. This diagram is drawn for the maximum strain developed in FRP sections during loading time. As can be seen in the diagram, the maximum compressive strain is 19 and the tensile strain is 23.9 mm.

In Figure 46, the contour of the von Mises stress created in the I-shaped supports of the B-4 model is drawn. As seen in the figure, the highest von Mises stress created is equal to 191.6 MPa and the lowest von Mises stress is equal to 1.25 MPa.

Figure 47 shows the von Mises stress contour created in the FRP sections of the B-4 deck. As can be seen in the

figure, the highest von Mises stress created in FRP sections is equal to 131.3 MPa and the lowest von Mises stress is equal to 1 MPa.

7. Conclusion

As can be seen in models 2 and 4 where the length of the deck spans is reduced, the amount of stress created in the FRP sections of the deck is greatly reduced. Also, in models 2 and 4, where the length of the deck openings has been reduced, the amount of strain created in the FRP sections of the deck has been greatly reduced. Therefore, it can be concluded that by reducing the length of the deck span in bridges with FRP box sections, the amount of stress and strain of the deck is reduced.

The compared stresses in trapezoidal FRP sections under traffic and earthquake loading show that in models 3 and 4, where the loading is in the form of an earthquake, the amount of stress created in the FRP sections of the deck has increased greatly. As in models 3 and 4, where the loading is in the form of an earthquake, the amount of strain created in the FRP sections of the deck has increased greatly. Therefore, it can be concluded that in bridges with trapezoidal FRP sections, the amount of deck stress and strain depends on the type of loading rather than the length of the span and the type of loading. By comparing the stress of trapezoidal and boxy FRP sections under traffic loading, it can be seen that in the model with boxy section and longer opening length, the amount of stress created in the FRP sections of the deck is higher than the rest of the models. Also, the strain of trapezoidal and boxy FRP sections under traffic loading has been compared. As can be seen, in the model with a boxy cross-section and longer opening length, the amount of strain created in the FRP sections of the deck is higher than the rest of the models. Therefore, it can be concluded that the stress and strain created in box sections is more than trapezoidal sections.

Comparing the stress of trapezoidal and boxy FRP sections under earthquake loading shows that in the boxy model with 3 openings, the amount of stress created in the FRP sections of the deck is much less than the rest of the models. Also, comparing the strain of trapezoidal and boxy FRP sections under earthquake loading, as can be seen in the boxy model with 3 openings, the amount of strain created in the FRP sections of the deck is much less than the rest of the models.

Acknowledgments

References

[1] Zhou, Aixi. Stiffness and strength of fiber reinforced polymer composite bridge deck systems. Diss. Virginia Polytechnic Institute and State University, 2002.

[2] Liu, Zihong. Testing and analysis of a fiber-reinforced polymer (FRP) bridge deck. Diss. Virginia Tech, 2007.

[3] Camata, Guido, and P. Benson Shing. Evaluation of GFRP Deck Panel for the O'Fallon Park Bridge. No. CDOT-DTD-R-2004-2,. Colorado Department of Transportation, Research Branch, 2004.

[4] Davalos, Julio F., et al. "Modeling and characterization of fiber-reinforced plastic honeycomb sandwich panels for highway bridge applications." Composite structures 52.3-4 (2001): 441-452.

[5] American Association of State Highway and Transportation Officials (AASHTO), "Specifications for Highway Bridges", Washington, 17th Edition, 2010

[6] Japan Road Association. "Reference for Seismic Retrofit of Existing Highway Bridges." Maruzen, Tokyo, Japan (1998).

[7] Karbhari, Vistasp M. "Materials considerations in FRP rehabilitation of concrete structures." Journal of materials in civil engineering 13.2 (2001): 90-97.